

Solid-state formation of lithium ferrites from mechanically activated $\text{Li}_2\text{CO}_3\text{--Fe}_2\text{O}_3$ mixtures

V. Berbenni^{a,*}, A. Marini^a, P. Matteazzi^b, R. Ricceri^b, N.J. Welham^c

^aCSGI, Dipartimento di Chimica Fisica dell'Università di Pavia, 27100 Pavia, Italy

^bCSGI, Dipartimento di Scienze e Tecnologie Chimiche dell'Università di Udine, 33100 Udine, Italy

^cMineral Science, Murdoch University, South Street, Murdoch, WA 6150, Australia

Received 5 January 2002; accepted 12 April 2002

Abstract

The formation of lithium ferrites (LiFe_5O_8 and LiFeO_2) from mechanically activated mixtures of $\text{Li}_2\text{CO}_3\text{--Fe}_2\text{O}_3$ has been studied using thermal analysis (TGA, DSC), evolved gas analysis (TG/FT-IR), X-ray powder diffraction (XRD), scanning electron microscopy (SEM) and particle size analysis. It is shown that mechanical activation of the precursors considerably enhances the reactivity of the solid system analysed and makes it possible to obtain reaction products with a much lower expense of thermal energy. In particular, lithium ferrites can be obtained at temperatures at least 160 °C lower than those necessary in the absence of mechanical activation. Moreover, both the microstructure and the allotropic ratio of the products, as well as the reaction path, are affected by mechanical activation. © 2002 Elsevier Science Ltd. All rights reserved.

Keywords: Ferrites; Microstructure; Milling; Powders-solid state reaction; Thermogravimetry

1. Introduction

Lithium ferrites (LiFe_5O_8 and LiFeO_2) have attracted considerable interest due to their potential technological applications. LiFeO_2 has been proposed as cathodic material in rechargeable lithium batteries, due to its lower toxicity and cost^{1,2} with respect to LiNiO_2 and LiCoO_2 . The spinel phase LiFe_5O_8 is a ferrimagnetic compound which has been used in the microwave field due to its square hysteresis loop and high Curie temperature. Several papers have appeared dealing with the electrical, magnetic and structural properties of lithium ferrites prepared by different methods.^{3–5} Their solid-state synthesis has been examined by Karagedov et al.⁶ who reported that the rate of formation was dependent on the thermal and/or mechanical history of the precursor and on the heating system used to perform the reaction. In previous work of ours,^{7,8} the formation of lithium ferrites was studied starting from Li_2CO_3 and from different iron precursors such as Fe_2O_3 , $\text{FeC}_2\text{O}_4 \cdot 2\text{H}_2\text{O}$ and $\text{Fe}_2(\text{C}_2\text{O}_4)_3 \cdot 6\text{H}_2\text{O}$.

However, new methods of materials synthesis have received attention in recent years. In particular, conventional thermally-driven solid-state reactions have a tendency to yield coarse grained agglomerated powders with compositional inhomogeneities.⁹ To overcome these deficiencies, interest has been focused on low temperature synthetic routes such as coprecipitation, sol-gel synthesis, alkoxide hydrolysis, hydrothermal reactions and citrate routes. These synthesis procedures often require annealing of the precursors at a high temperature to allow the formation of the desired phases and in many cases high-purity inorganic or organometallic chemicals have to be employed as starting materials (which are more expensive than the widely available oxides and carbonates). An alternative procedure is represented by a mechanically activated synthesis route, which basically consists of a high-energy ball milling process, where repeated fracture and welding events arising from impact and compression between the milling medium and the particles result in the production of homogeneously mixed fine powders. Mechanochemistry was initially developed for the synthesis of intermetallic compounds and alloys.¹⁰ Later it was used to prepare various magnetic and nanocrystalline materials.^{11,12} Recently, mechanical activation has been applied to

* Corresponding author. Tel.: +39-382-507-211; fax: +39-382-507-575.

E-mail address: berbenni@matsci.unipv.it (V. Berbenni).

improve the reactivity of the starting composition so that the desired compound is formed at a reduced annealing temperature.¹³

This work examines the formation of lithium ferrites (LiFe_5O_8 and LiFeO_2) from mixtures of Li_2CO_3 and Fe_2O_3 which have been previously subjected to mechanical activation by high energy milling. The study has been performed by means of high resolution thermogravimetric analysis (HRes TGA), differential scanning calorimetry (DSC), evolved gas analysis by coupled thermogravimetric analysis and Fourier transform infrared spectroscopy (TGA/FT-IR), X-ray powder diffraction (XRPD) and scanning electron microscopy (SEM).

2. Experimental procedure

2.1. Starting products and sample preparation

The starting chemicals were purchased from Aldrich Chimica (Italy): Li_2CO_3 purum (99%) and Fe_2O_3 (nominally +99% hæmatite, although magnetite was detected by XRPD).

Mixtures of composition $X_{\text{Li}}=0.16$ (LiFe_5O_8) and $X_{\text{Li}}=0.50$ (LiFeO_2) (X_{Li} =lithium cationic fraction) were prepared by weighing the appropriate amounts of the two components. A sample of each mixture was simply mixed for 10 min using an agate mortar and pestle. These samples are considered to be simple physical mixtures (i.e. unactivated). About 20 g of the different sample compositions were milled for 2 and 5 h in a high energy, high capacity vibratory ball mill (grinding balls to powder ratio 10:1, carbon steel balls),¹⁴ in air atmosphere.

2.2. Experimental techniques

Thermogravimetric analysis (TGA) was performed using a 2950 thermogravimetric analyser connected to a TA 5000 data station (TA Instruments, USA) equipped with Thermal Solutions[®] software. About 20 mg of each sample was heated under a nitrogen flow of 100 ml/min to 850 °C. Both conventional thermogravimetry (i.e. at constant heating rate of 2 °C/min) and high resolution thermogravimetry¹⁵ using a dynamic rate approach were used.

Conventional TGA measurements have also been performed by connecting a thermobalance (TGA 951 thermogravimetric analyser by DuPont de Nemours, USA) to a FT-IR spectrometer (FT-IR spectrometer Mod. 730 by Nicolet, USA equipped with Omnic[®] software). The measurements were performed up to 650 °C at a heating rate of 5 °C/min. Flowing nitrogen (40 ml/min) was used to carry the gaseous products from the thermobalance into the FT-IR gas cell (which

was maintained at 240 °C throughout the TGA measurement). The spectra of the evolved gases were obtained by fast fourier transform of 16 co-added interferograms collected at 8 cm^{-1} resolution. Specific absorbance chemigrams of the likely gaseous products (H_2O and CO_2) have been reconstructed at the end of the run by means of the Nicolet Series[®] software.

The mechanically activated samples were also analysed using a differential scanning calorimeter (DSC, Model 2920 by TA Instruments, USA, connected to a TA5000 data station equipped with Thermal Solutions[®] software). About 20 mg of each sample were heated up to 650 °C at 2 °C/min, in open platinum pans and under a nitrogen flow of 60 ml/min.

Samples of both unreacted and reacted mechanically activated mixtures were examined by X-ray diffractometry (Bruker Model D5005 powder diffractometer with a monochromated copper source) in order to identify the different phases. Measurements were made over the range $2\theta=20\text{--}70^\circ$ using a 3 s counting time per 0.03° step. The mean crystal size has been calculated by the method described elsewhere¹⁶ using the full width at half maximum (FWHM) of the X-ray peaks corrected for instrumental broadening and taking into account strain effects.

Samples of both mechanically activated and physical mixtures (either reacted and unreacted) were examined by a scanning electron microscope (SEM, Model Stereoscan 200 by Cambridge, UK). The samples having been previously sputtered under vacuum with gold metal.

The particle size distribution of the samples was examined using a Coulter LS100 Laser Diffractometer (0.4–900 μm simultaneous range): the measurements were performed in a water medium so that no information on water soluble Li_2CO_3 could be obtained.

3. Results and discussion

3.1. Milled samples characterisation

Fig. 1 shows the XRPD patterns of the different milled samples, where the $\alpha\text{-Fe}_2\text{O}_3$ markers (JCPDS file No. 33–0664) are reported. It can be seen that the only peaks that cannot be assigned to $\alpha\text{-Fe}_2\text{O}_3$ are the weak and broad peaks present at $2\theta \approx 21.5^\circ$, 30.5° and 32° . While the first and the last of them can be assigned to Li_2CO_3 (JCPDS file No. 22–1141) and are only barely visible in the milled LiFeO_2 precursors (i.e. lithium richer samples), that at $2\theta \approx 30.5^\circ$ could correspond to the 100% intensity peak of Fe_3O_4 (JCPDS file No. 19–0689) which was present in the starting iron oxide. The apparent absence of lithium carbonate in the LiFe_5O_8 mixture is due to a combination of its low volume fraction and preferential amorphisation of the

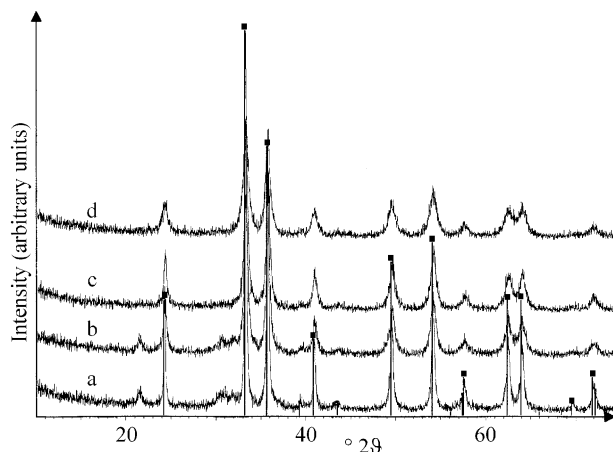


Fig. 1. XPRD patterns of the different milled precursors. (a) LiFeO_2 2 h milling; (b) LiFeO_2 5 h milling; (c) LiFe_5O_8 2 h milling; (d) LiFe_5O_8 5 h milling. The markers of Fe_2O_3 are reported (JCPDS card No. 33-0664).

softer of the two phases (Li_2CO_3), which has been noted previously.^{17,18}

The XRPD peaks of $\alpha\text{-Fe}_2\text{O}_3$ are broad, indicating that a reduction of crystal size had occurred as a consequence of milling. From the line broadening, the crystal size of $\alpha\text{-Fe}_2\text{O}_3$ in the milled samples has been estimated (see Table 1). It is clear that in the iron rich sample (LiFe_5O_8) the haematite has reached an equilibrium crystallite size within 2 h, but for the lower iron sample (LiFeO_2) crystallite size is apparently still being reduced after 5 h. Presumably, the larger fraction of lithium carbonate in the LiFeO_2 mixture is mitigating the damage to the haematite.

The particle size distribution of the physical mixture and milled samples were measured. However, since lithium carbonate was soluble in the water medium used, the results refer to Fe_2O_3 only. Fig. 2a reports the particle size distribution of the as-received haematite. It can be seen that the distribution is centred at $\approx 3 \mu\text{m}$ with a shoulder towards higher particle size. The LiFeO_2 precursor (2 h milling time, Fig. 2b) has a distribution centred at $\approx 1 \mu\text{m}$ with a smaller shoulder towards higher particle dimensions. The same precursor milled for 5 h (Fig. 2c) has a distribution centred at $\approx 0.8 \mu\text{m}$, again with a shoulder towards higher particle size. The reported trend stresses the efficiency of the milling process in both reducing particle size and in

reagglomerating particles. The agglomeration effect is enhanced by increasing the milling time.

Fig. 2d shows that the LiFe_5O_8 sample mixture milled 2 h has a distribution centred at $\approx 0.9 \mu\text{m}$ but it also shows a significant fraction of particles in the 10–60 μm range. The same precursor milled for 5 h (Fig. 2e) has a distribution centred at $\approx 0.8 \mu\text{m}$ with the most significant fraction of particles in the 4–100 μm range. Thus it seems that the efficiency of the agglomeration in the milling process is enhanced in the LiFe_5O_8 precursor. The greater agglomeration of the LiFe_5O_8 was not unexpected since the probability of two Fe_2O_3 particles contacting and rewelding is greater than in the LiFeO_2 mixture.

Fig. 3 shows a micrograph of the “ LiFeO_2 ” physical mixture Fig. (3a) along with those of the same mixture milled for 2 h (Fig. 3b) and 5 h (Fig. 3c). As would be expected milling for 2 h milling involves a drastic reduction in the particle size. The most striking feature of Fig. 3c is the considerable extent of rewelding that has occurred by extending the milling to 5 h. The SEM micrographs of LiFe_5O_8 physical mixture and of the samples milled 2 and 5 h showed very similar results.

3.2. Milled samples reactivity

3.2.1. LiFeO_2 precursor—non-isothermal experiments

Fig. 4 shows the TGA scans obtained on samples of LiFeO_2 precursors which were unmilled (4a), milled 2 h (4b) and 5 h (4c). From these, the following can be proposed:

- A slight mass loss process occurs in the milled samples, between room temperature and about 250 °C that does not occur in the physical mixture;
- The main process in the milled samples is a single-step mass loss between about 250 °C and 600 °C. It has to be noted that this mass loss is completed at a temperature well below that where spontaneous decomposition of Li_2CO_3 occurs ($\approx 640 \text{ °C}$). On the contrary, the mass loss process of the physical mixture starts at about 430 °C and comprises two steps that ended at about 620 °C and 800 °C respectively;
- By increasing the milling time the process slightly shifts towards lower temperatures;
- The mass loss of the physical mixture (its mean value over 6 measurements) is slightly higher than that of the milled samples and coincides, within the experimental error, with the expected value.

The mean total mass loss of the 2 h milled sample was $-18.58 \pm 0.05\%$ (mean and standard deviation of five measurements) and $-18.45 \pm 0.08\%$ for the 5 h milled sample. The mean values are the same within the

Table 1
Crystal size of the milled samples

Sample	Crystal size (nm)
LiFeO_2 precursor 2 h milled	34
LiFeO_2 precursor 5 h milled	17
LiFe_5O_8 precursor 2 h milled	14
LiFe_5O_8 precursor 5 h milled	14

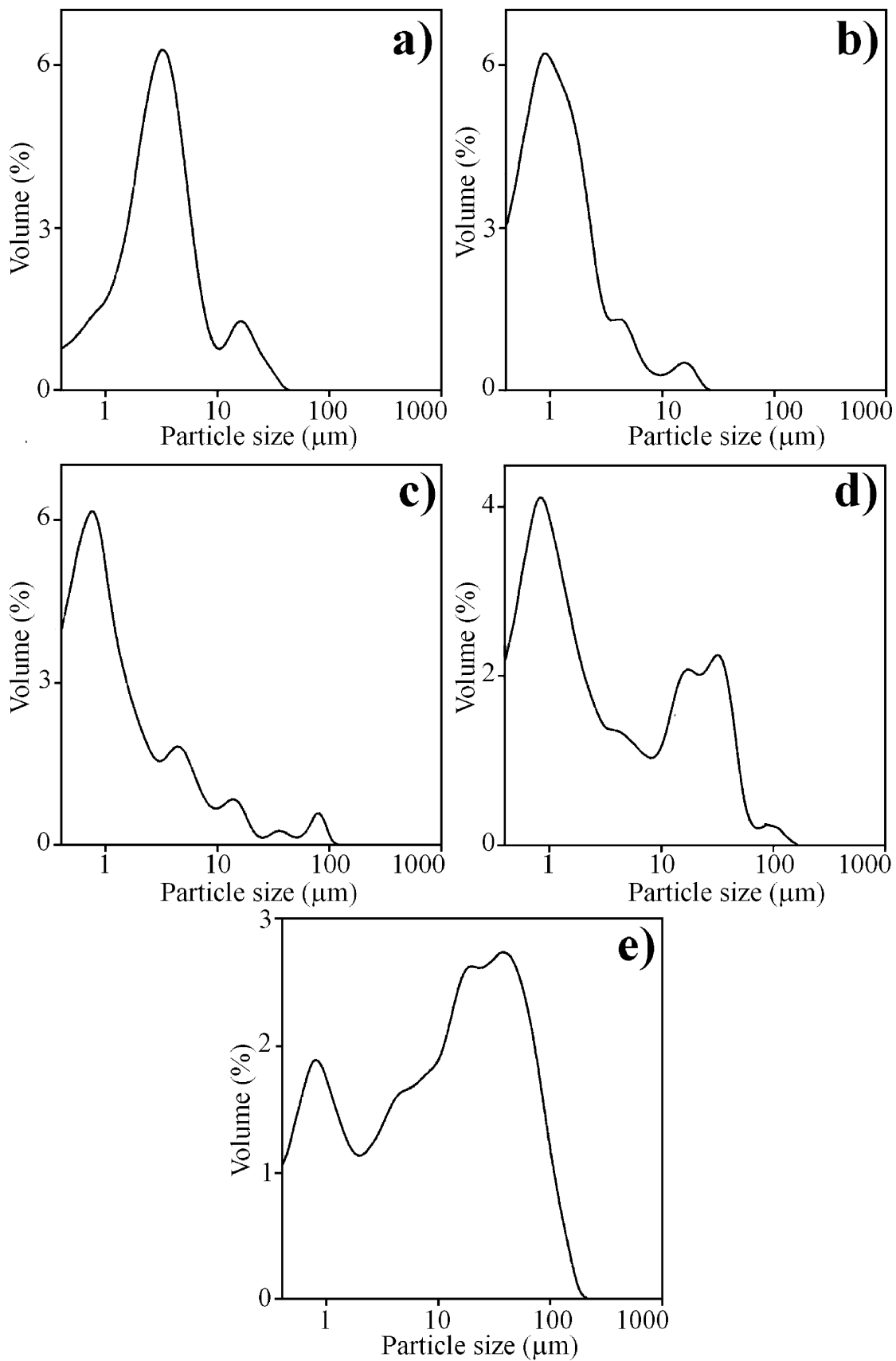


Fig. 2. Particle size distribution of the different precursors. (a) original haematite; (b) LiFeO_2 2 h milling; (c) LiFeO_2 5 h milling; (d) LiFe_5O_8 2 h milling; (e) LiFe_5O_8 5 h milling.

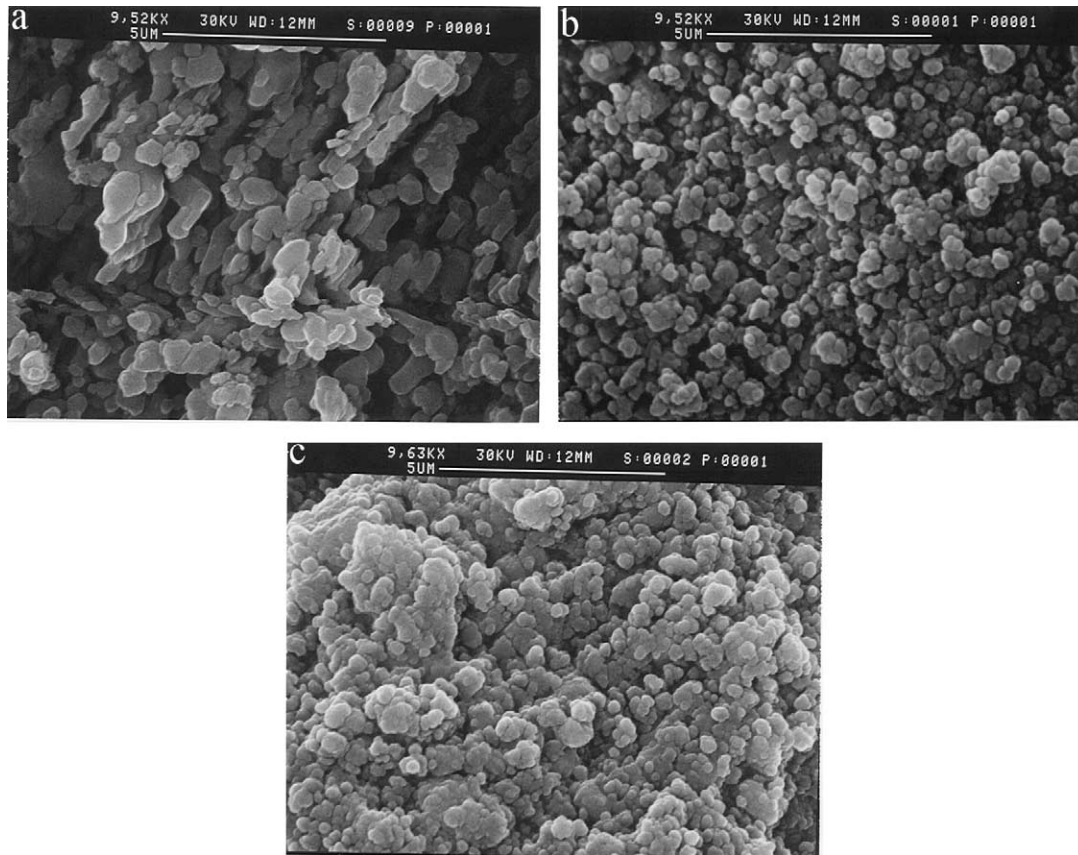


Fig. 3. SEM micrographs of the different precursors. (a) LiFeO₂ physical mixture; (b) LiFeO₂ 2 h milling; (c) LiFeO₂ 5 h milling.

experimental error, and both of them are lower than the expected value of -18.84% calculated as the mass loss of the process $\text{Li}_2\text{CO}_3 + \text{Fe}_2\text{O}_3 \rightarrow 2\text{LiFeO}_2 + \text{CO}_2$.

One can hypothesise that these positive experimental-expected differences are in general due to the impurities in the starting powders. However, the origin of the mentioned discrepancies could also be found in the weight gain arising from the oxidation of Fe₃O₄ impurity whose presence has been verified by XRPD in the as-received $\alpha\text{-Fe}_2\text{O}_3$ and/or by the oxydation of Fe which

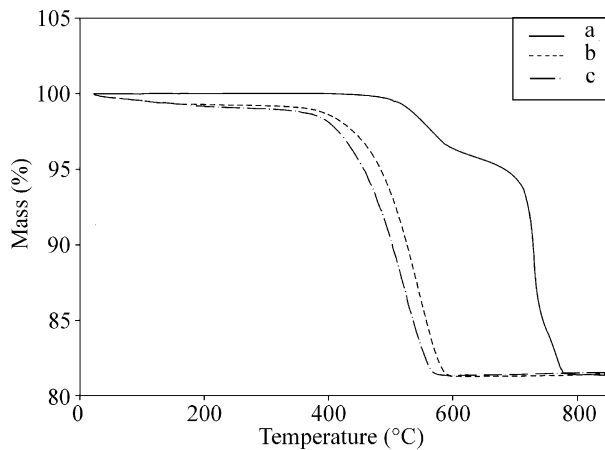


Fig. 4. TGA thermograms of: (a) LiFeO₂ physical mixture; (b) LiFeO₂ 2 h milling; (c) LiFeO₂ 5 h milling.

comes from the milling media. The decreasing trend of the mass loss with increasing milling time, makes this last hypothesis the most likely one.

It has been previously said that the mass loss process starts in the milled samples at room temperature although the starting chemicals do not contain adsorbed volatile substances (such as water and/or carbon dioxide). Coupling TG analysis with FT-IR spectroscopy has determined which gases evolved over this early stage of mass loss (up to 250 °C). Fig. 5 shows the coadded IR spectra of the gases evolved from TGA between room temperature and 250 °C for 5 h milled sample (the sample milled 2 h shows the same behavior). Only carbon dioxide is evolved over the entire temperature range (see the upward pointing bands at $\approx 2200\text{ cm}^{-1}$ and $\approx 670\text{ cm}^{-1}$). On the contrary the absorbance bands pointing downward refer to water and mean that less water is present in the system than at the beginning of the run and this rules out the release of water from the milled samples. The carbon dioxide released up to 250 °C can only come from Li₂CO₃ decomposition in the mechanically activated samples. To support that the low temperature mass loss is due to an early Li₂CO₃ decomposition, pure Li₂CO₃ was milled for 2 and 5 h and then analyzed by TGA. For both milling times a continuous mass loss process was evident from room temperature up to 250 °C (2.4 and 3.6% for the samples

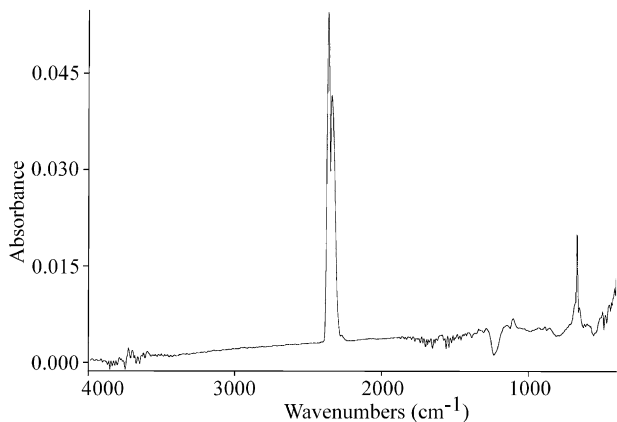


Fig. 5. Coadded TG/FT-IR spectra of the gases evolved in the temperature range 25–250 °C from LiFeO₂ precursor milled for 5 h.

milled 2 and 5 h, respectively).¹ This proves that high energy milling greatly activates Li₂CO₃ decomposition. On the contrary, we cannot prove if the low temperature Li₂CO₃ decomposition is followed by LiFeO₂ formation. As a matter of fact, XRPD patterns of milled samples heated up to 250 °C, does not show any significant difference to those of the as-milled samples. However it must be taken into account that:

- the amount of LiFeO₂ possibly formed is near to the detection limit of XRPD;
- It is likely that LiFeO₂ formed at such lower temperatures would be of amorphous nature.

To go deeper into this point the progress in the reaction was also followed by taking XRPD patterns of samples of 5 h milled powder that had been heated up to 400, 450, 500 and 550 °C. From the relevant mass loss results, the expected% conversion to LiFeO₂ was 8.3 at 400 °C, 19.1 at 450 °C, 50.0 at 500 °C and 88.2 at 550 °C. However, the LiFeO₂ reflections were barely visible only at the highest temperature and there was only indirect reaction evidence at lower temperatures with the diminishing intensity of the hematite peaks. Therefore, although it is clear that lithium ferrite is produced at all temperatures it is in a microcrystalline or even amorphous form which cannot be revealed by XRPD until it has started to undergo crystal growth at higher temperatures.

The reaction in the milled samples was also examined by DSC. The relevant DSC thermogram shows an endothermic peak (onset temperature 416 °C, maximum temperature 550 °C) with an enthalpy of +47.3 kJ/mol LiFeO₂. DSC measurement were previously performed,⁷ under the same experimental conditions, on a physical mixture of the same composition and resulted

¹ The as-received Li₂CO₃ does not show any mass loss up to $T \approx 640$ °C.

in an endothermic peak with an enthalpy of +55.6 kJ/mol LiFeO₂. If it is assumed that the 8.3 kJ/mol difference in enthalpy is due to slow ferrite formation at temperatures below the peak onset then approximately 14.9% was formed below 416 °C. This value is reasonable, given the above calculated conversions at 400 and 450 °C were 8.3% and 19.1% respectively.

Another indication of a different reaction route in the milled samples can be found in the XRPD patterns. Only the cubic α -LiFeO₂ (JCPDS file No.17-0938) forms in the reacted physical mixture,⁷ while a mixture of all the possible LiFeO₂ phases [cubic α , tetragonal β (JCPDS file No. 17-0936) and tetragonal γ (JCPDS file No. 17-0937)] forms when heating the milled powders at 2 °C/min up to 700 °C (see Fig. 6).

Finally Fig. 7 shows the SEM micrographs of the reaction product of the physical mixture (Fig. 7a) and the 2 h (Fig. 7b) and 5 h (Fig. 8c) milled samples after all of them were recovered at the end of TGA runs of Fig. 4. It can be seen that both milled samples yield a very similar microstructure characterised by round particles and a somewhat large extent of particle welding in the longer milled samples (Fig. 7c) as expected. In contrast, the microstructure of the physical mixture is completely different showing elongated particles (Fig. 7a).

3.2.2. Isothermal experiments

LiFeO₂ formation from mechanically activated precursors has also been examined by performing isothermal experiments. Namely, the 5 h milled samples have been heated into the TGA apparatus up to fixed temperatures (350, 400, 450 and 500 °C, that are all well below the Li₂CO₃ onset of spontaneous decomposition) where they have been maintained for different times.

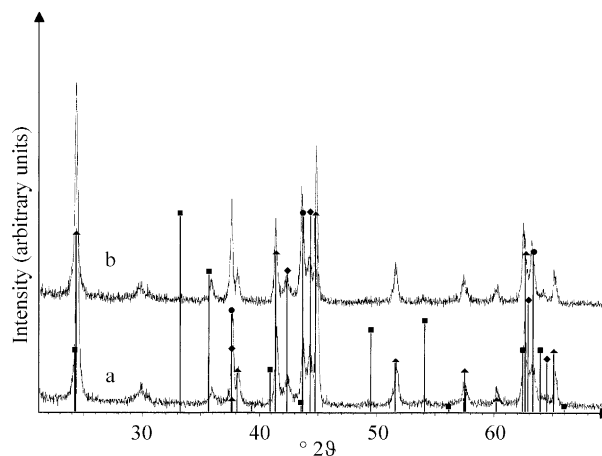


Fig. 6. XRPD patterns of the reacted (i.e. heated up to 700 °C) LiFeO₂ milled precursors: (a) 2 h milling; (b) 5 h milling. The markers of Fe₂O₃ (squares, JCPDS card No. 33-0664), α -LiFeO₂ (circles, JCPDS card No. 17-0938), β -LiFeO₂ (lozenges, JCPDS card No. 17-0936) and γ -LiFeO₂ (triangles, JCPDS card No. 17-0937) are indicated.

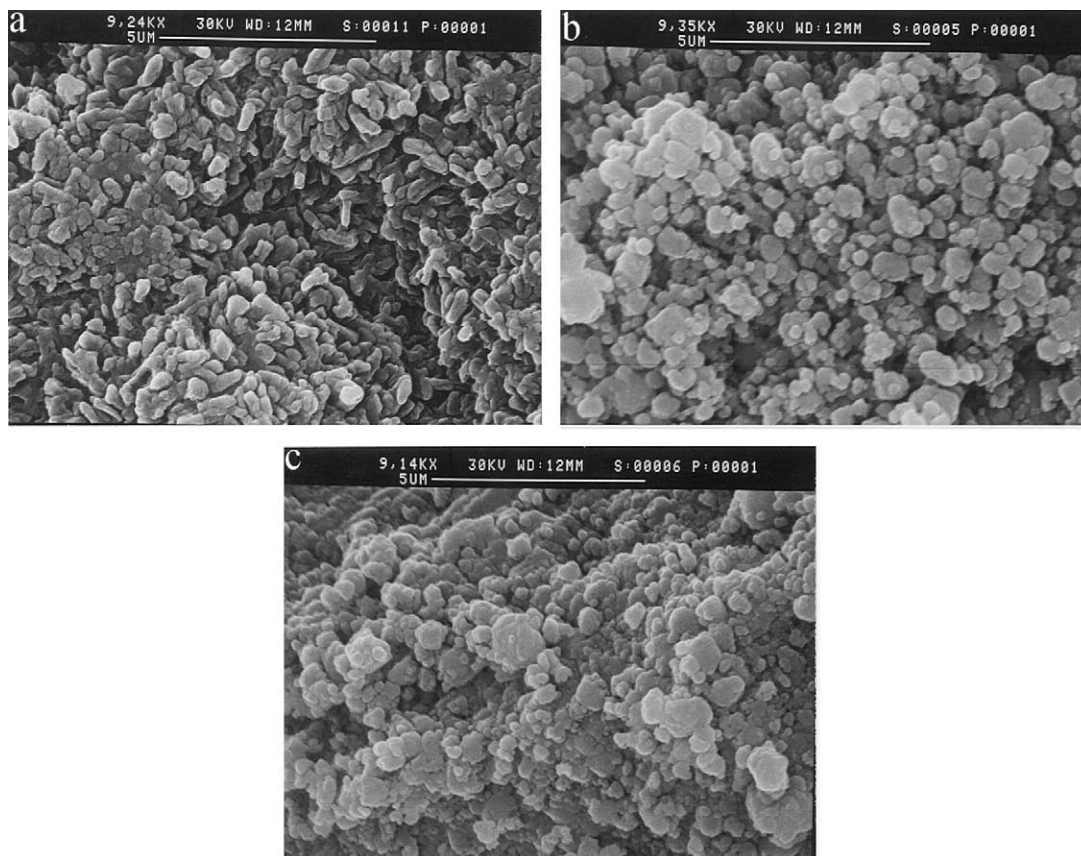


Fig. 7. SEM micrographs of the reacted precursors. (a) LiFeO_2 physical mixture; (b) LiFeO_2 2 h milling; (c) LiFeO_2 5 h milling.

The mass loss data show that 50% reaction extent is reached in 1100 min at 400°C while only about 12 min are needed at 500°C . The mass losses at all temperatures have been shown to fit the three-dimensional diffusion equation proposed by Jander.¹⁹ The fit is quite satisfactory: the Jander equation, which applies to diffusion controlled reactions in a spherical particle, is followed for the entire temperature range and from the Arrhenius equation an activation energy of 95.7 kJ/mol LiFeO_2 has been obtained. The actual physical meaning of the activation energy is obviously questionable, however it is clear that the reaction in the mechanically activated sample has a single stage whose rate is diffusion determined. The physical mixture showed (Fig. 4) the presence of two stages, the first of which was completed at about 650°C (i.e. about the onset temperature of Li_2CO_3 spontaneous decomposition) and involved a mass loss close to that expected for the complete formation of LiFe_5O_8 . It could be thought that the reaction in the physical mixture proceeds in two consecutive stages, formation of LiFe_5O_8 followed by reaction with excess Li_2CO_3 to yield LiFeO_2 . To investigate this point, we performed TGA measurements on mixtures milled under less intense conditions (planetary mill, agate balls, 5 min and 5 h milling). Two stages were still present, the first one, though starting at lower temperatures than in the unmilled physical mixture, was still completed by

about 650°C and showed a mass loss which increased with milling time. This experimental fact suggests that the formation of LiFeO_2 is not due to sequential reactions but due to a different extent of intimate mixing between lithium carbonate and iron oxide. Such intimate mixing increases with milling time, so shifting towards lower temperature the Li_2CO_3 decomposition, which in turn results from its reaction with Fe_2O_3 .

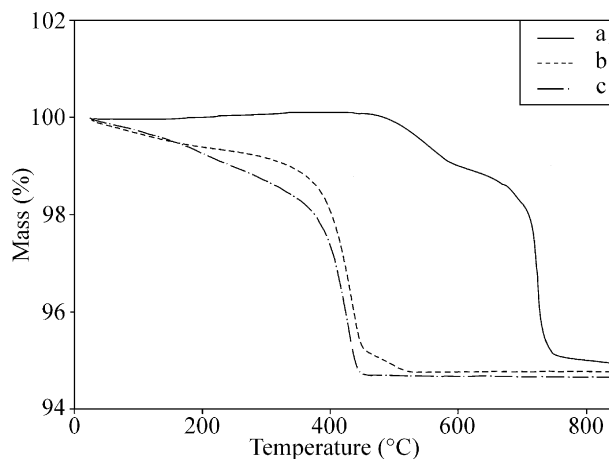
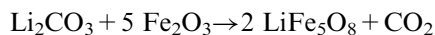


Fig. 8. TGA thermograms of (a) LiFe_5O_8 physical mixture; (b) LiFe_5O_8 2 h milling; (c) LiFe_5O_8 5 h milling.

3.2.3. LiFe_5O_8 precursor—non isothermal experiments

Fig. 8 reports the TGA scans obtained on the physical mixture (Fig. 8a) and samples milled for 2 h (Fig. 8b) and 5 h (Fig. 8c). The main differences between the mechanically activated samples and the physical mixture are:

- The presence of a stage of mass loss between room temperature and about 200 °C. In the physical mixture, on the contrary, a slight mass increase takes place up to 425 °C that is likely due to Fe_3O_4 impurity oxidation;
- A single-step mass loss occurs between about 250 °C and 540 °C for the sample milled 2 h and between 200 °C and 470 °C after milling for 5 h. Both end temperatures are well below the onset temperature of Li_2CO_3 spontaneous decomposition (≈ 640 °C). In the physical mixture, after the mentioned mass increase up to 425 °C, the mass loss process is constituted by two stages ending at 620 and 770 °C respectively. A further mass loss, even if a minor one, occurs up to 850 °C (maximum temperature of the TGA run).
- The mean total mass loss of the sample milled for 2 h was $-5.15 \pm 0.06\%$, essentially the same as the $-5.07 \pm 0.09\%$ for the 5 h milled powder. It can be concluded that the following reaction (for which the expected mass loss is -5.04%) is taking place:



As in the case of LiFeO_2 precursors, TG/FT-IR measurements have shown that carbon dioxide is

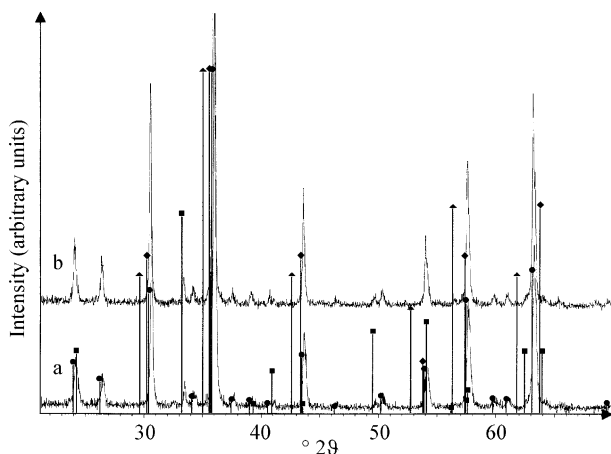


Fig. 9. XRPD patterns of the reacted (i.e. heated up to 650 °C) LiFe_5O_8 milled precursors: (a) 2 h milling; (b) 5 h milling. The markers of Fe_2O_3 (squares, JCPDS card No. 33-0664), $\alpha\text{-LiFe}_5\text{O}_8$ (circles, JCPDS card No. 38-0259), $\beta\text{-LiFe}_5\text{O}_8$ (lozenges, JCPDS card No. 17-0114) and $\delta\text{-LiFe}_5\text{O}_8$ (triangles, JCPDS card No. 17-0117) are indicated.

the main gaseous product released over the mass loss up to 250 °C.

A DSC thermogram of the sample milled for 5 h showed an endothermic peak (onset 384 °C, peak 429 °C) with an enthalpy of $+26.5$ kJ/mol LiFe_5O_8 . The already mentioned previous work reported for a physical mixture of the same composition (under the same experimental conditions) enthalpy change of $+70.2$ kJ/mol LiFe_5O_8 .⁷ This is equivalent to 62% of the reaction occurring prior to the onset of the endotherm; the TGA measurements indicate that about half of the reaction had already occurred at 385 °C.

XRPD of the products (Fig. 9) obtained by heating the milled samples at 2 °C/min up to 650 °C showed both α (cubic JCPDS file No. 38-0259) and β (cubic disordered modification, JCPDS file No. 17-0114) LiFe_5O_8 phases are present, $\delta\text{-LiFe}_5\text{O}_8$ (JCPDS file No. 17-0117) did not apparently form.²

Fig. 10 shows SEM micrographs of the reaction product (maximum temperature 850 °C) obtained from the physical mixture (Fig. 10a) and the powders milled for 2 h (Fig. 10b) and 5 h (Fig. 10c) after they were recovered at the end of TG runs of Fig. 8. It can be seen that the two reacted milled samples show a similar microstructure where the rounded particles are a little smaller than those obtained starting from the milled LiFeO_2 precursor (Fig. 7b and c). This is likely due to the lower reaction temperatures for the LiFe_5O_8 milled precursors. A completely different microstructure can be observed in the reacted physical mixture.

3.2.4. LiFe_5O_8 precursor—iso thermal experiments

LiFe_5O_8 formation from mechanically activated precursors has also been examined by performing isothermal experiments. Samples milled for 5 h were heated up to 300, 350, 375 and 400 °C (all below Li_2CO_3 decomposition) where they have been maintained for different times. The data shows that 50% completion of the reaction was reached after 1350 min at 300 °C and only ~ 7 min at 400 °C. In this case the mass loss data at all temperatures fitted the Ginstling–Brounshtein complex diffusion equation which holds for diffusion controlled reactions in a quite complex shaped particle.¹⁹ From the Arrhenius equation an activation energy of 97.0 kJ/mol LiFe_5O_8 was obtained, which is essentially the same activation energy as for LiFeO_2 formation. This implies that the rate-determining step was the same for both reactions.

² There is also a slight excess of $\alpha\text{-Fe}_2\text{O}_3$ (JCPDS file No. 33-0664) which may suggest formation of minor amounts of LiFeO_2 .

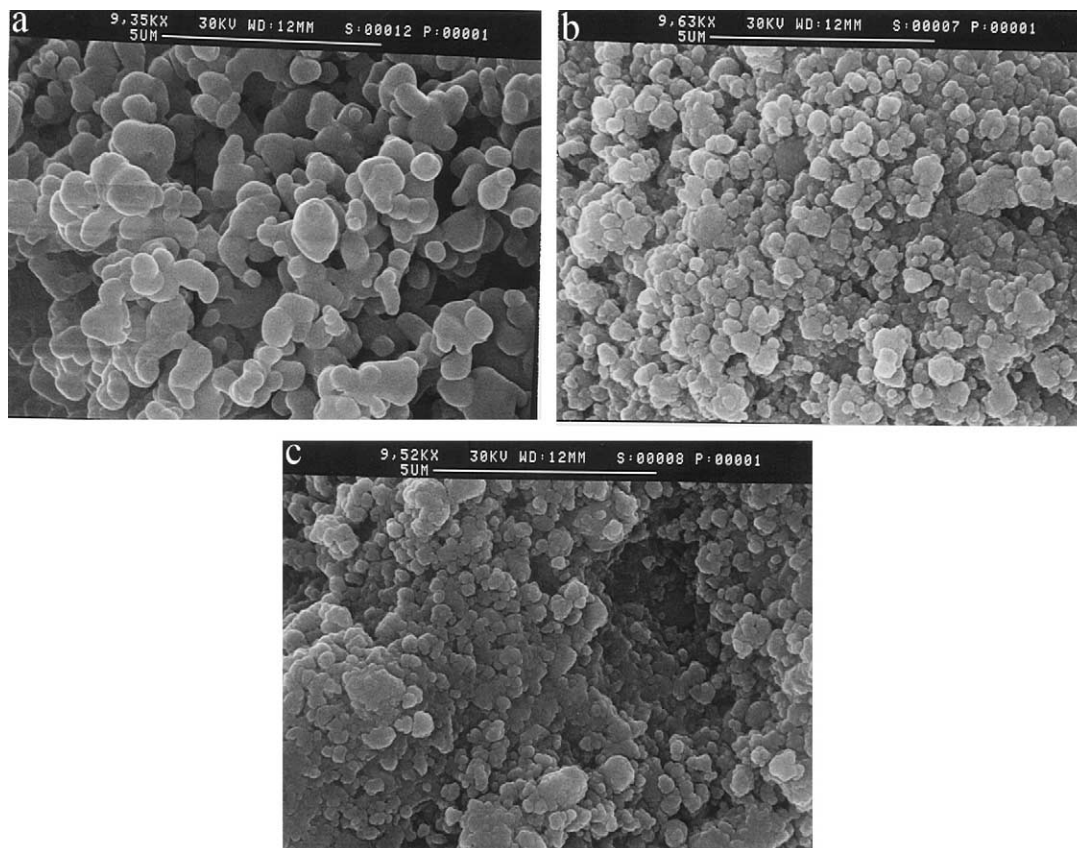


Fig. 10. SEM micrographs of the reacted precursors. (a) LiFe_5O_8 physical mixture; (b) LiFe_5O_8 2 h milling; (c) LiFe_5O_8 5 h milling.

4. Conclusions

Mechanical activation of the precursors considerably enhances the reactivity of the solid system analysed and makes it possible to obtain reaction products at a considerably lower temperature: lithium ferrites (LiFeO_2 and LiFe_5O_8) can be obtained at temperatures at least 200°C lower than in the absence of mechanical activation. Moreover, both the microstructure and the allotropic ratio of the products, as well as the reaction path, are affected by mechanical activation. Namely:

- the microstructure of the lithium ferrites formed starting from the milled sample is quite different from that of the ferrites obtained from physical mixtures;
- while only $\alpha\text{-LiFeO}_2$ and $\alpha\text{-LiFe}_5\text{O}_8$ phases form when starting from the stoichiometric physical mixtures respectively, a mixture of α , β and $\gamma\text{-LiFeO}_2$ and of α and $\beta\text{-LiFe}_5\text{O}_8$ forms when starting from mechanically activated samples of corresponding composition;
- the formation of both lithium ferrites from the mechanically activated powders shows only a single reaction stage whose rate is diffusion controlled. The activation energy values are nearly the same for both reactions though the kinetic

model is slightly different in the two cases due to some differences in the particle shapes.

References

1. Dahn, J. R., Von Sacken, U. and Michal, C. A., Structure and electrochemistry of $\text{Li}_{1\pm y}\text{NiO}_2$ and a new Li_2NiO_2 phase with the $\text{Ni}(\text{OH})_2$ structure. *Solid State Ionics*, 1990, **44**, 87–97.
2. Sakurai, Y., Arai, H., Okada, S. and Yamaki, J., Low temperature synthesis and electrochemical characterization of LiFeO_2 cathodes. *J. Power Sources*, 1997, **68**, 711–715.
3. Ramachandran, N. and Biswas, A. B., Magnetic and Mossbauer studies on $\alpha\text{-Fe}_2\text{O}_3\text{-Li}_2\text{O}$ System. *J. Solid State Chem.*, 1979, **30**, 61–64.
4. Shirane, T., Kanno, R., Kawamoto, Y., Takeda, Y., Takano, M., Kamiyama, T. and Izumi, F., Structure and physical properties of lithium iron oxide, LiFeO_2 , synthesized by ionic exchange reaction. *Solid State Ionics*, 1995, **79**, 227–233.
5. Tabuchi, M., Ado, K., Kobayashi, H., Matsubara, I., Kageyama, H., Wakita, M., Tsutsui, S., Nasu, S., Takeda, Y., Masquelier, C., Hirano, A. and Kanno, R., Magnetic properties of metastable lithium iron oxides obtained by solvothermal/hydrothermal reaction. *J. Solid State Chem.*, 1998, **141**, 554–561.
6. Karagedov, G. R., Konovalova, E. A., Boldyrev, V. V. and Lyachov, N. Z., Influence of reagent biography and reaction conditions on kinetics of lithium ferrite synthesis. *Solid State Ionics*, 1990, **42**, 147–151.
7. Berbenni, V., Marini, A. and Capsoni, D., Solid state reaction study of the system $\text{Li}_2\text{CO}_3\text{-Fe}_2\text{O}_3$. *Z. Naturforsch.*, 1998, **53a**, 997–1003.

8. Berbenni, V., Marini, A., Bruni, G. and Riccardi, R., Solid state reaction study in the systems $\text{Li}_2\text{CO}_3\text{-FeC}_2\text{O}_4\cdot 2\text{H}_2\text{O}$ and $\text{Li}_2\text{CO}_3\text{-Fe}_2(\text{C}_2\text{O}_4)_3\cdot 6\text{H}_2\text{O}$. *Thermochim. Acta*, 2000, **346**, 115–132.
9. Amin, A., Spears, M. A. and Kulwicki, B. M., Reaction of anatase and rutile with barium carbonate. *J. Am. Ceram. Soc.*, 1983, **66**, 733–736.
10. Benjamin, J. S., Mechanical alloying. *Sci. Am.*, 1976, **234**, 40–48.
11. Ding, J., Miao, W. F., McCormick, P. G. and Street, R., Mechanochemical synthesis of ultrafine Fe powder. *Appl. Phys. Lett.*, 1995, **67**, 3804–3806.
12. Giri, A. K., amorphous materials prepared through crystallization by ball milling. *Adv. Mater.*, 1997, **9**, 163–166.
13. Welham, N. J., Formation of micronised WC from scheelite. *Materials Sci. Eng., A*, 1998, **248**, 230–237.
14. Basset, D., Matteazzi, P. and Miani, F., Designing a high energy ball-mill for synthesis of nanophase materials in large quantities. *Materials Sci. Eng. A*, 1993, **168**, 149–152.
15. Berbenni, V., Marini, A. and Bruni, G., Thermogravimetric study of the dehydration process of α -cyclodextrin: comparison between conventional and high-resolution TGA. *Thermochim. Acta*, 1998, **322**, 137–151.
16. Matteazzi, P. and Le Caër, G., Synthesis of nanocrystalline alumina-metal composites by room temperature ball milling of metal oxides and aluminum. *J. Am. Ceram. Soc.*, 1992, **75**, 2749–2755.
17. Weeber, A. W. and Bakker, H., Amorphization by ball milling. *A review Physica B*, 1988, **153**, 93–135.
18. Welham, N. J., Mechanical activation of the solid state reaction between Al and TiO_2 . *Materials Sci. Eng. A*, 1998, **255**, 81–89.
19. Keatch, C. J. and Dollimore, D. The Operation of the Thermobalance. A. Kinetic Data from Isothermal Experiments; in An Introduction to Thermogravimetry. Heyden, 1975, pp. 57–81.